Int. J. Multiphase Flow Vol. 19, No. 2, pp. 391–395, 1993
Printed in Great Britain.

0301-9322/93 $6.00 + 0.00

BRIEF COMMUNICATION

VAPORIZATION WAVE STRUCTURE OF DENSE BIMODAL SPRAYS

S. LEE
Korea Institute of Nuclear Safety, P.O. Box 16, Daeduk-Danji, Taejon, South Korea

(Received 7 July 1992; in revised form 18 November 1992)

INTRODUCTION

In the practical combustion of liquid fuel sprays, dense droplet sprays are prevalent and the conditions experienced by discrete droplets may be quite different from those obtained in a single droplet analysis, notably due to droplet interaction. A series of group combustion models for the structure and burning characteristics of liquid fuel sprays has been developed by Chiu and coworkers (Suzuki & Chiu 1971; Chiu & Liu 1977; Chiu *et al.* 1982), and the spray combustion models are classified according to a group combustion number G. Correa & Sichel (1982a, b) performed an asymptotic analysis for small ε values and obtained external sheath combustion results that agree well with those of Chiu and coworkers. Where ε is the square of the ratio of the two lengths, i.e. the thickness of a vaporization wave at the edge of the cloud and the initial cloud radius. In the limiting cases, $\varepsilon \ll 1$, the interior of the cloud remains in undisturbed saturated equilibrium and droplet evaporation only occurs across a thin front or vaporization wave of thickness at the edge of the cloud, in analogy to a single droplet.

Most of the work on spherical clouds has been limited to monodisperse sprays. However, a knowledge of the behavior of clouds with a generalized droplet size distribution may be important in determining cloud lifetime, wave speed and other vaporization characteristics. Because of the complication of developing analytical solutions for a generalized distribution function, the problem has been simplified by considering a bimodal distribution in order to qualitatively investigate the effect of the size distribution on spray clouds.

FORMULATION

A spherical cloud with a bimodal droplet size distribution in a quiescent atmosphere is considered. The cloud has an initial radius R_i and contains both smaller droplets of initial radius a_{1i} with number density n_1 and larger droplets of initial radius a_{2i} with number density n_2. Then the ratios m_{La}, defined as the ratio of the initial mass of the liquid to the air, and m_{12}, defined as the ratio of the initial mass of the smaller droplets to the larger droplets, will be important parameters in this analysis. The following assumptions have been used in the analysis:

(i) The cloud is initially in saturated equilibrium at some reference temperature T_r.
(ii) The details of the initial heat-up processes, during which the cloud interior reaches saturated equilibrium, are not considered.
(iii) Fick's law of diffusion is valid.
(iv) The pressure is constant everywhere.
(v) The Lewis number Le is taken to be unity.

The nondimensionalized equations for the conservation of mass, species and energy in the cloud interior, including the source terms due to droplet varporization, can be expressed as follows using the characteristic length R_i, velocity α_r/R_i and time R_i^2/α_r:

$$\varepsilon \frac{\partial \bar{\rho}}{\partial \bar{t}} + \frac{\varepsilon}{\bar{r}^2} \frac{\partial}{\partial \bar{r}} [\bar{r}^2 \bar{\rho} \bar{v}] = \frac{\beta_1 \bar{a}_1 + \bar{a}_2}{1 + \beta_3} \ln(1 + \theta), \quad [1]$$

$$\varepsilon \frac{\partial}{\partial \bar{t}}[\bar{\rho}(\hat{Y}_r - Y)] + \frac{\varepsilon}{\bar{r}_2}\frac{\partial}{\partial \bar{r}}\left\{\bar{r}^2\left[\bar{\rho}\bar{v}(\hat{Y}_r - Y) + \frac{\partial Y}{\partial \bar{r}}\right]\right\} = \frac{\beta_1 \bar{a}_1 + \bar{a}_2}{1+\beta_3}\ln(1+\theta), \quad [2]$$

$$\varepsilon \frac{\partial}{\partial \bar{t}}(\bar{\rho}\bar{u}) + \frac{\varepsilon}{\bar{r}^2}\frac{\partial}{\partial \bar{r}}\left\{\bar{r}^2\left[\bar{\rho}\bar{v}\theta - \frac{\partial \theta}{\partial \bar{r}}\right]\right\} = -\frac{\beta_1 \bar{a}_1 + \bar{a}_2}{1+\beta_3}\ln(1+\theta), \quad [3]$$

$$\frac{\partial \bar{a}_1^2}{\partial \bar{t}} = -2\frac{R_i^2}{a_{1i}^2}\frac{\rho_r}{\rho_L}\ln(1+\theta) \quad [4]$$

and

$$\frac{\partial \bar{a}_2^2}{\partial \bar{t}} = -2\frac{R_i^2}{a_{2i}^2}\frac{\rho_r}{\rho_L}\ln(1+\theta), \quad [5]$$

where ε is a small parameter which is expressed as

$$\varepsilon = [4\pi(\beta n_1 a_{1i} + n_2 a_{2i})R_i^2]^{-1}$$

and $\beta = a_{1i}^2/a_{2i}^2$, $\beta_1 = n_1 a_{1i}/n_2 a_{2i}$, $\beta_3 = m_{12}$, $\bar{a}_1 = a_1/a_{1i}$, $\bar{a}_2 = \bar{a}_2/a_{2i}$, $\theta = c_p(T - T_r)/L$, $\hat{Y}_r$ = fuel vapor mass fraction at saturated condition, L = latent heat of vaporization, α = thermal diffusity of the gas phase, $\bar{\rho}$ = gas phase density and c_p = gas phase specific heat.

Equations [4] and [5] are obtained from the standard quasi-steady single droplet theory using the local cloud conditions as the ambient conditions for each droplet. Assuming that the vaporization front or wave at the edge of the cloud has a thickness of order $\varepsilon^{\nu}R_i$, the following stretched inner variables are now introduced to describe the flow within the wave:

$$r^w = \frac{R - r}{R_i \varepsilon^{\nu}}, \quad r < R_i$$

$$r^w = \frac{t}{R_i/U_r}, \quad [6]$$

where $R = R_i = U_t$ and U_r is vaporization wave speed. The wave-fixed coordinates are used to shift the singular boundary condition to the origin of the inner coordinates.

For $\varepsilon \ll 1$, vaporization occurs across a thin vaporization wave at the edge of the cloud. However, this wave will now have a bimodal structure. If it is assumed that the evaporation of the individual droplets follows the "d^2-law" and if the time rate of change of the square of the droplet radius is the same for both smaller or larger droplets (i.e. equal evaporation constant), there is a region near the edge of the cloud where all the smaller droplets are completely vaporized, represented as $0 \leqslant r^w \leqslant r_b^w$, while both large and small droplets will be present in the inner region $r_b^w \leqslant r^w \leqslant \infty$. Here r^w is the stretched inner variable within the evaporation wave. The wave structure is governed by two different sets of equations for each of these regions. With the substitution of the expanded inner variables and the Galilean transformation [6], [1]–[5] will be divided into two regions, to lowest order, as follows:

(i) region 1: $0 \leqslant r^w \leqslant r_b^w$ (only larger droplets exist),

$$\frac{d\phi_0^w}{dr^w} = \frac{a_{20}^w}{1+\beta_3}\theta_0^w, \quad [7]$$

$$\frac{d}{dr^w}\left\{\phi_0^w \hat{Y}_r + \frac{dY_0^w}{dr^w}\right\} = \frac{a_{20}^w}{1+\beta_3}\theta_0^w, \quad [8]$$

$$\frac{d}{dr^w}\left\{\frac{d\theta_0^w}{dr^w}\right\} = \frac{a_{20}^w}{1+\beta_3}\theta_0^w, \quad [9]$$

$$(a_{10}^w)^2 = 0, \quad [10]$$

$$\frac{d(a_{20}^w)^2}{dr^w} = \gamma_0 \theta_0^w; \quad [11]$$

and

(ii) region 2: $r_b^w \leqslant r^w \leqslant \infty$ *(both smaller and larger droplets exist),*

$$\frac{d\phi_0^w}{dr^w} = \frac{\beta_1 a_{10}^w + a_0^w}{1+\beta_3}\theta_0^w, \tag{7a}$$

$$\frac{d}{dr^w}\left\{\phi_0^w \hat{Y}_r + \frac{dY_0^w}{dr^w}\right\} = \frac{\beta_1 a_{10}^w + a_{20}^w}{1+\beta_3}\theta_0^w, \tag{8a}$$

$$\frac{d}{dr^w}\left\{\frac{d\theta_0^w}{dr^w}\right\} = \frac{\beta_1 a_{10}^w + a_{20}^w}{1+\beta_3}\theta_0^w, \tag{9a}$$

$$\frac{d(a_{10}^w)^2}{dr^w} = \frac{1}{\beta}\gamma_0\theta_0^w, \tag{10a}$$

$$\frac{d(a_{20}^w)^2}{dr^w} = \gamma_0\theta_0^w; \tag{11}$$

where the superscript w represents the condition within the cloud and the subscript 0 represents the zeroth-order solution, and $\phi = \bar{\rho}\bar{v}$.

Here the region $r^w \leqslant r_b^w$ represents the region near the edge of the cloud where all the smaller droplets are completely vaporized, and the parameter γ_0, which is given by

$$\gamma_0 = \frac{2R_i\lambda}{a_{2i}^2\rho_L c_p U_0},$$

plays the role of an eigenvalue which determines the propagation speed U_0 of the wave and λ is gas phase thermal conductivity.

Boundary conditions at the cloud edge may be obtained from the conservation of mass, species and energy across the wave (Lee 1988).

To integrate equations (7)–(11), direct step-by-step integration was initiated from $r^w = 0$ with an assumed value of the eigenvalue γ_0. The final solution was then obtained by guessing values of the eigenvalue until the correct value satisfying the matching conditions within the cloud was determined.

Results have been obtained for a bimodal cloud with 10 and 100 μm octane droplets at an ambient temperature 500 K and an ambient oxidizer mass fraction 0.23. A typical example of the structure of the vaporization wave of the octane cloud for $m_{12} = 0.01$ and 1.0 at $m_{La} = 4.25$ is shown in figure 1. Here m_{La} is defined as the ratio of liquid to the air mass and m_{12} is defined as the ratio of smaller to larger droplet mass. It is clearly shown that the temperature and concentration gradients are very steep near the cloud edge and approach zero toward the cloud interior, and both the smaller and larger droplets are completely evaporated at the edge of the cloud and approach saturation conditions at the cloud interior. For bimodal sprays, smaller droplets evaporate faster than larger droplets because of the higher surface-to-volume ratio. Thus, as the ratio of the mass of the smaller to the larger droplets m_{12} increases, the evaporation rate of the larger droplets at the cloud edge is smaller and r_b^w, where all the smaller droplets are completely vaporized is closer to the edge of the cloud.

Analysis of the region inside the cloud provided information on the profiles of temperature and fuel vapor mass fraction only in terms of $\theta_0^w/\theta_0^w(0)$ and $Y_0^w/\theta_0^w(0)$. In order to complete the solution and determine $\theta_0^w(0)$, the temperature at the edge of the cloud, it now becomes necessary to determine a solution for the region outside the cloud.

The dimensionless equations to zeroth order and the boundary conditions in the inner region from following the same procedure as Correa & Sichel (1982a). The results can be summarized as follows:

$$\frac{d\xi^2}{dt} = -\frac{6\varepsilon\lambda}{a_{2i}^2\rho_L c_p}\ln(1+\theta_\infty)$$

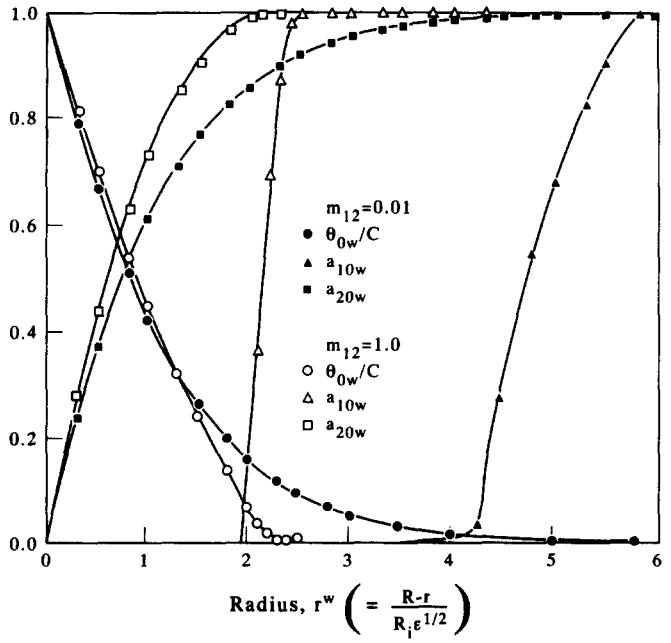

Figure 1. Effect of m_{12} in a vaporizing cloud for $m_{La} = 4.25$.

or

$$\xi^2 = 1 - \frac{1}{\tau_c}, \qquad [12$$

where ξ is defined as R/R_i and the cloud lifetime τ_c is given by

$$\tau_c = \frac{2\pi(n_1 a_{1i}^3 + n_2 a_{2i}^3)R_i^2 \rho_L c_p}{3\lambda \ln(1+\theta_\infty)}. \qquad [13]$$

Equation (12) shows that the cloud with a bimodal spray also obeys a "d^2-law" like the monodisperse cloud. As in the case of the monodisperse droplet cloud, the behavior of lowest-order quasi-steady cloud with a bimodal droplet size distribution shows several analogies to single droplet theory. After cloud equilibrium is reached, the vaporization characteristics are determined not by the droplet size distribution but by the ratio of the initial mass of the liquid to air and by the initial air temperature. Thus, if the mass ratio m_{La} is the same, the vaporization characteristics of bimodal sprays such as the cloud lifetime and the wave speed are the same as those of a monodisperse spray (Correa & Sichel 1982a).

CONCLUSIONS

The lowest-order quasi-steady cloud behavior for dense, bimodal sprays shows that the cloud radius is found to decrease according to a "d^2-law" in analogy with single droplet theory, although with a modified vaporization constant. It can be concluded that while the particle size distribution will influence the structure of the vaporization wave which forms at the edge of the cloud, the total vaporization time is independent of the size distribution but depends only on the mass of spray per unit volume, the liquid properties and the ambient temperature far away from the cloud. Although these results have been derived for a bimodal size distribution, it appears likely that the above conclusions will remain valid for more general distributions; however, this generalization still requires rigorous proof. The result is not surprising and indicates that in the dense sprays the vaporization rate depends on the total heat flux into the cloud surface and the total amount of liquid which must be vaporized.

This analysis could be extended to find higher-order solutions in order to evaluate the effects of unsteadiness and be continued to evaluate the behavior of clouds with generalized droplet size distributions.

REFERENCES

CHIU, H. H. & LIU, T. M. 1977 Group combustion of liquid droplets. *Combust. Sci. Technol.* **17,** 127–142.

CHIU, H. H., KIM, H. Y. & CROKE, E. J. 1982 Internal group combustion of liquid droplets. In *Proc. 19th Int. Symp. on Combustion*, The Combustion Institute, pp. 971–980.

CORREA, S. M. & SICHEL, M. 1982a The boundary layer structure of a vaporizing fuel clouds. *Combust. Sci. Technol.* **28,** 121–130.

CORREA, S. M. & SICHEL, M. 1982b The group combustion of a spherical cloud of monodisperse fuel droplets. In *Proc. 19th Int. Symp. on Combustion*, The Combustion Institute, pp. 981–991.

LEE, S. 1988. Evaporation and combustion of dense fuel droplets with a bimodal droplet size distribution. Ph.D. dissertation, Univ. of Michigan, Ann Arbor, MI.

SUZUKI, T. & CHIU, H. H. 1971 Multi-droplet combustion of liquid propellants. In *Proc. 9th Int. Symp. on Space Technol. Sci.*, pp. 145–154.